

ENHANCED ENZYMATIC HYDROLYSIS AND CHANGES IN STRUCTURE OF CELLULOSE REGENERATED WITH IONIC LIQUIDS

QIUJIN LI,^{*, **, *****} WEI QI,^{**, ****, *****} RONGXIN SU^{**, ****, *****} and ZHIMIN HE^{**, *****}

^{*}*School of Textiles, Tianjin Polytechnic University, Tianjin, 300387, China*

^{**}*State Key Laboratory of Chemical Engineering, School of Chemical Engineering and Technology, Tianjin University, Tianjin, 300072, China*

^{***}*Tianjin Key Laboratory of Membrane Science and Desalination Technology, Tianjin, 300072, China*

^{****}*Co-Innovation Center of Chemistry and Chemical Engineering of Tianjin, Tianjin, China*

^{*****}*Key Laboratory of Advanced Textile Composites (Tianjin Polytechnic University), Ministry of Education, Tianjin, 300387, China*

✉ *Corresponding author: Wei Qi, qiwei@tju.edu.cn*

Received October, 20, 2015

Two kinds of ionic liquids (ILs), 1-butyl-3-methylimidazolium chloride ([BMIM]Cl) and 1-allyl-3-methylimidazolium chloride ([AMIM]Cl), were synthesized to pretreat Whatman filter paper (WFP) for accelerating the enzymatic hydrolysis of cellulose. The hydrolysis rate of IL-pretreated cellulose was significantly enhanced, with a sugar conversion of nearly 100% (24 h). FTIR, XRD, SEM and molecular weight distribution (MWD) analyses verified that the hydrogen bonds and crystalline pattern of cellulose were destroyed after regeneration from ILs. The orderly and compact fibrillar morphologies of cellulose disappeared after IL-pretreatment, and, instead, a fault structure and small holes on the surface could be observed. The changes in the structure of cellulose played an essential role in the enhancement of enzymatic hydrolysis.

Keywords: cellulose, ionic liquid, enzymatic hydrolysis, sugar conversion, molecular weight, molecular weight distribution

INTRODUCTION

As part of the general biomass, cellulose is the most abundant resource in nature. Cellulose is a linear polysaccharide composed of D-anhydroglucopyranose linked by β -1,4-glucosidic bonds with the degree of polymerization (DP) from 100 to 20000.¹⁻³ Van der Waals forces⁴ and extensive hydrogen bonds⁵ afford cellulose a stiff molecular alignment and a structure consisting of highly crystalline sites connected by amorphous sites.

This results in a heterogeneous structure of cellulose and low accessibility to cellulases.^{3,6,7} Enzymatic hydrolysis of cellulose is the premise to produce ethanol fuel and other types of biomass energy. Cellulose hydrolysis suffers from low reaction rate and sugar conversion because of its insoluble and heterogeneous nature in aqueous solvents. The native crystalline structure of cellulose and lignin complexity are considered as two of the major

factors that restrict saccharification yields during enzymatic hydrolysis.^{5,8,9} Therefore, it is important to overcome the inherent highly ordered crystalline structure of cellulose by some feasible pretreatments.

Many methods of pretreatment have been employed to change the crystalline structure of cellulose, including biological, physical and chemical methods.¹⁰⁻¹² Herein, we focused on chemical methods, especially solvent pretreatment. Generally, concentrated acids were used to pretreat cellulose, such as sulphuric acid, nitric acid *etc.*¹³ Walseth *et al.*¹⁴ swelled cellulose in 85% phosphoric acid and the pretreated cellulose could be easily degraded by cellulases. From then on, phosphoric acid-swollen celluloses were widely studied.¹⁵⁻¹⁸ Zhang *et al.*^{19,20} dissolved cellulose in 83% phosphoric acid; the regenerated cellulose was amorphous and could be hydrolyzed to nearly 100% after 24 h. Kuo *et al.*²¹ pretreated cellulose with *N*-methylmorpholine-*N*-oxide (NMMO), and the regenerated cellulose was converted to glucose after 72 h.

Ionic liquids (ILs) are considered as “green solvent” for cellulose due to their low volatility, excellent dissolution ability and ease of recycling.²² Cellulose could completely dissolve in ionic liquids in large amounts under mild conditions.²³ Rogers *et al.*²⁴⁻²⁷ first reported that cellulose could be dissolved in ILs and studied deeply the dissolution and regeneration of cellulose in ILs. Heinze *et al.*²³ studied the dissolution of cellulose in different ILs, and reported that ILs could dissolve cellulose in high concentration without derivatization. Zhang *et al.*²⁸ studied the dissolution of cellulose in 1-allyl-3-methylimidazolium chloride ([AMIM]Cl). Wu *et al.*²⁹ reported that the solubility of cellulose in [AMIM]Cl was up to 10%. Dadi *et al.*³⁰ pretreated cellulose with 1-butyl-3-methylimidazolium ([BMIM]Cl), and the initial enzymatic hydrolysis rate improved approximately 50-fold after the pretreatment. Sun *et al.*³¹ pretreated cellulose with ionic liquids, and confocal Raman microscopy and confocal fluorescence microscopy were used to understand the mechanism of ionic liquid

pretreatment. Sun *et al.*³² studied the crystallinity of regenerated cellulose fiber and film produced by dissolving raw pulp into ionic liquid [BMIM]Cl, using the extrusion method. Liu *et al.*³³ reported [BMIM]Cl-pretreated cellulose for TEMPO-NaClO-NaBr oxidation had a higher production yield compared with ultrasonic and sodium hydroxide pretreatments. Ma *et al.*³⁴ synthesized cellulose phthalates from beet pulp cellulose and phthalic anhydride in [BMIM]Cl, which enhanced the degree of substitution greatly. Bodirlau *et al.*³⁵ suggested that the saccharification rate of *Asclepias syriaca* (As) fiber by cellulase in the presence of ionic liquids was significantly accelerated. Spiridon *et al.*³⁶ pretreated *Asclepias syriaca* seed floss and poplar seed floss by three kinds of ionic liquids. The hydrolysis kinetics and rates for the pretreated flosses were greatly enhanced. Cheng *et al.*³⁷ reported the influences of 1-ethyl-3-methyl imidazolium acetate ([C₂MIM][OAc]) on the cellulose crystalline structure in different feedstocks. For pure cellulose, the native crystalline structure (cellulose I) was a major factor impacting its saccharification process, yet for general biomass samples, lignin-carbohydrate complexes also effected the rate of cellulose hydrolysis.

After dissolution in ILs, cellulose could be easily regenerated by rapidly precipitating in an anti-solvent, such as water, ethanol *etc.* Due to the extraordinary dissolution ability and modest operating condition of ILs, cellulose regenerated from ILs has great potential in biomass refinery.

In this work, two kinds of ILs, 1-butyl-3-methylimidazolium chloride ([BMIM]Cl) and 1-allyl-3-methylimidazolium chloride ([AMIM]Cl), were synthesized to dissolve and regenerate Whatman filter paper (WFP). The sugar conversion of IL-pretreated WFP was significantly enhanced. The chemical structure, crystalline pattern and supramolecular morphology of regenerated WFP were characterized by Fourier transform infrared spectroscopy (FTIR), X-ray diffraction (XRD) and scanning electron microscopy (SEM). The molecular weight distribution (MWD) of regenerated WFP during enzymatic hydrolysis

was also obtained by size exclusion chromatography (SEC). Hereafter, the reason for accelerated enzymatic hydrolysis of regenerated WFP was discussed. This work reveals the profound impact of IL pretreatment on changes in the structure of cellulose, as well as the enzymatic process.

EXPERIMENTAL

Materials

Whatman No. 1 filter paper (WFP, cut by a paper punch prior to use) was obtained from Unite Stars Biotechnology Co. Ltd. (Tianjin, China). *N*-methylimidazole was purchased from J&K Chemical Co. Ltd. (Beijing, China). Cellulase GC220 was obtained from Genencor International Inc. (CA, U.S.A.) and Novozyme 188 (β -glucosidase) was obtained from Sigma Inc. Lithium chloride (LiCl) was stored in a desiccator before use. *N*, *N*'-dimethylacetamide (DMAc) and all other chemicals were purchased from Concord Technology (Tianjin, China) without further purification.

Synthesis of [BMIM]Cl and [AMIM]Cl

N-methylimidazole (100 mL) and butyl chloride (160 mL) at a molar ratio of 1:1.2 were added to a round-bottomed flask fitted with a reflux condenser and stirred for 24 h at 80 °C. After vacuum distillation to remove the unreacted chemical reagents, the white solid, [BMIM]Cl, was obtained. *N*-methylimidazole (100 mL) and allyl chloride (200 mL) at a molar ratio of 1:1.25 were added to a round-bottomed flask fitted with a reflux condenser and stirred for 8 h at 55 °C. After vacuum distillation, the amber liquid, [AMIM]Cl, was obtained.

Pretreatment and regeneration of cellulose

10% (w/w) cellulose solutions were prepared by dissolving 5 g cellulose (shred WFP pieces) in 50 g [BMIM]Cl or [AMIM]Cl, stirred at 120 °C for 1~2 h. After the complete dissolution of cellulose, about 5-fold volume water was rapidly added to each cellulose solution for precipitating cellulose from ILs. The samples were filtered to obtain the regenerated celluloses, which were washed with water for five times to remove the ILs completely. After lyophilization, the regenerated cellulose could be used for further experiments.

Scanning electron microscopy (SEM)

The morphology of celluloses was analyzed by

scanning electron microscopy (SEM, Hitachi S-3500N) at an accelerating voltage of 20 kV. The samples were sputter-coated with Au prior to measurement.

Fourier transform infrared spectroscopy (FTIR)

The original or regenerated cellulose samples were lyophilized and laminated with potassium bromide. The FTIR spectra were recorded using Nicolet 560E.S.P.

X-ray diffraction (XRD)

The crystalline index (C_rI) of cellulose was determined by X-ray diffraction (XRD, PANalytical X'Pert Pro) using $\text{CuK}\alpha$ radiation ($\lambda = 1.789 \text{ \AA}$) at 30 kV and 30 mA with a scan rate of 12 °/min from 5° to 50°. The crystalline index (C_rI) was calculated by the method proposed by Segal.³⁸

Enzymatic hydrolysis of cellulose

Enzymatic hydrolysis was carried out in 10 mL of citric acid buffer (50 mM, pH 4.8), containing regenerated cellulose (50 g/L) and cellulase (40 FPU GC220 and 60 IU Novozyme 188 β -glucosidase per gram of cellulose) in an agitation shaker at 150 rpm and 50 °C. The hydrolysates were withdrawn at different time intervals and heated to 100 °C for 10 min to denature cellulases,³⁹ followed by separation through filtration. After separation, the liquid phase was measured for the released amount of soluble sugars, and the insoluble residue was washed by distilled water three times and lyophilized prior to measurement of molecular weight. Enzymatic hydrolysis of original cellulose was also performed for comparison.

High performance liquid chromatography (HPLC)

The released amount of sugars after the enzymatic hydrolysis of cellulose was measured by HPLC, using an Aminex HPX-87H (Bio-Rad) column operated at a flow rate of 0.6 mL/min with 0.01 M H_2SO_4 as mobile phase. Detection was undertaken using an RI-71 differential refractometer (SHODEX, Japan). The HPLC system was operated at 65 °C. The injection volume was 20 μL . Hydrolysate samples were filtrated through a 0.45 μm nylon membrane prior to analysis. The released amount of sugars was the total quantity of the cellobiose and glucose.

Size exclusion chromatography (SEC)

According to the reference,⁴⁰ cellulose residues at

different reaction time intervals of enzymatic hydrolysis were dissolved in LiCl/DMAc and their molecular weights were obtained using SEC. The molecular weights of original celluloses were also tested as control. These tests were carried out on a SEC system consisting of an Agilent 1100 isocratic pump (Agilent Technologies, Waldbronn, Germany), a Rheodyne 7725i injector loop of 100 μL and three columns, including PLgel 5 μm Guard, PLgel 5 μm MIXED-C and PLgel 5 μm 500 \AA (Polymer Laboratories, Shropshire, UK). The column temperature was thermostated at 80 $^{\circ}\text{C}$. Detection was undertaken using an RI-71 differential refractometer (SHODEX, Japan). The samples were filtered through 0.45 μm nylon membrane prior to analysis.

RESULTS AND DISCUSSION

Changes in structure of IL-regenerated WFP

Influence of ionic liquids on morphology of WFP

The morphologies of original and regenerated WFP are shown in Figure 1. Original WFP (Fig. 1A) has some large

cellulosic fibers with an orderly structure, accompanied by some fibrils. After IL-pretreatment, the native structures of WFP were lost. The intact fibrillar form completely disappeared, and was replaced by a filamentous surface with a loose structure, accompanied by little pores, as observed for [AMIM]Cl-treated (Fig. 1B) and [BMIM]Cl-treated WFP (Fig. 1C). It indicated that the ordered structure of cellulose was destroyed through dissolving in ILs.

Characterization of celluloses by FTIR

FTIR spectra of original and regenerated (from two different ionic liquids, [AMIM]Cl and [BMIM]Cl) WFP are shown in Figure 2. There are no significant changes in the spectra between original and regenerated WFP and no new peaks appeared in the spectra of the regenerated WFP, which suggests that no chemical reaction occurred during the dissolution process in ILs.²⁸

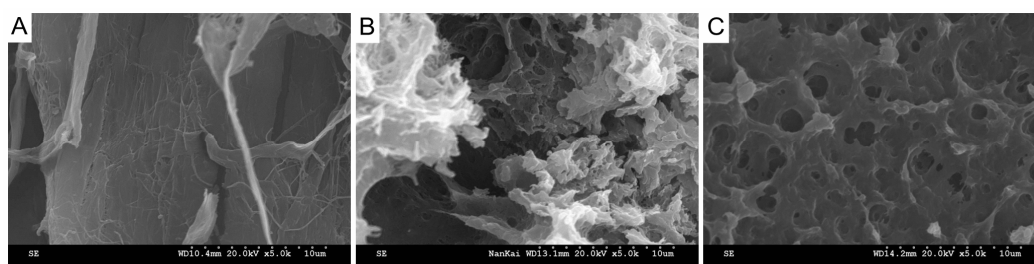


Figure 1: SEM images of WFP (A), WFP regenerated from [AMIM]Cl (B), and from [BMIM]Cl (C) (scale bar = 10 μm)

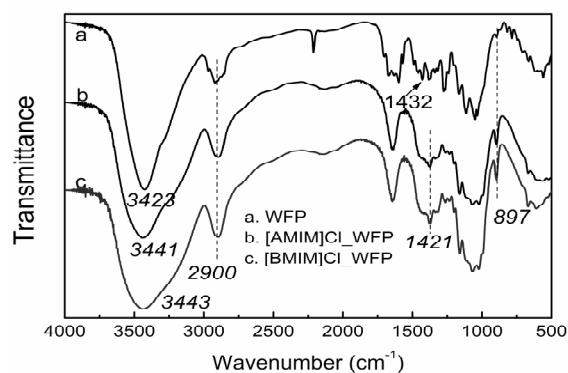


Figure 2: FTIR spectra of original WFP (a) and WFP regenerated from ionic liquids [AMIM]Cl (b) and [BMIM]Cl (c)

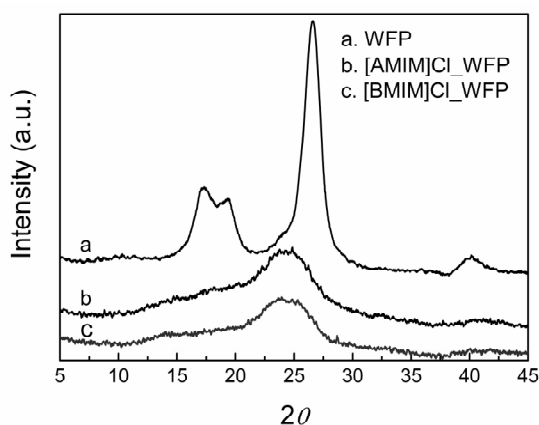


Figure 3: XRD curves of original WFP (a) and WFP regenerated from ionic liquids [AMIM]Cl (b) and [BMIM]Cl (c)

The bands located around 3400 cm^{-1} are the characteristic absorption of the O-H vibration of cellulose, which indicate the hydrogen bonding between the molecular chains of cellulose. Comparing to the original WFP, this peak shifted to higher wavenumbers (from 3423 cm^{-1} to 3441 cm^{-1} and 3443 cm^{-1}), indicating the decrease in hydrogen bonding of regenerated WFP. It demonstrated hydrogen bonds of cellulose chains were destroyed after dissolving in ILs. The peaks at 1432 cm^{-1} assigned to CH_2 vibration of the original WFP shifted to lower wavenumber of 1421 cm^{-1} , suggesting the destruction of the intramolecular hydrogen bonds in cellulose molecules alignments.^{28,41} The peak at 897 cm^{-1} , indicating C-O stretching of the amorphous cellulose, increased significantly after IL-pretreatment, which implied the transformation of cellulose from a crystalline to an amorphous pattern after IL-pretreatment.

Crystalline patterns of celluloses

XRD curves of original and regenerated WFP are shown in Figure 3. For original WFP, the peaks at $2\theta = 17.31^\circ$ and 19.36° belong to the 101 plane, while the peaks at $2\theta = 26.62^\circ$ and $2\theta = 40.15^\circ$ belong to the 002 plane and the 040 plane, respectively. They are the typical pattern of cellulose I.⁴² After regeneration from [BMIM]Cl and [AMIM]Cl, the IL-pretreated

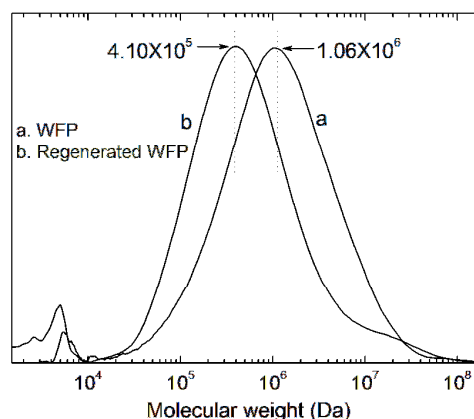


Figure 4: Molecular weight distributions of original and [BMIM]Cl-pretreated WFP

WFP exhibited a broad diffraction peak at a range of $2\theta = 14.5^\circ \sim 25.1^\circ$, which is the characteristic crystalline pattern of cellulose II.⁴³ Besides, the intensity of the diffraction peaks of regenerated WFP was much weaker than that of the original samples, indicating a significant decrease in crystallinity. It suggested that the extensive hydrogen bonding in cellulose molecules was significantly broken and the crystalline pattern was transformed from cellulose I to cellulose II after IL-regeneration.⁴⁴

Molecular weight distribution of original and regenerated WFP

As shown in Figure 4, [BMIM]Cl-pretreated WFP was taken as an example to exhibit the change in molecular weight distribution (MWD) of cellulose. After [BMIM]Cl pretreatment, MWD of WFP shifted from $\text{MW} = 1.06 \times 10^6$ to 4.10×10^5 , indicating that some crystalline region or cross-linked structures in original WFP was destroyed. It might indicate that the high crystalline region has larger MW than the amorphous region.

To summarize, considering the SEM, FTIR, XRD and SEC results comprehensively, the intact morphologies of original WFP were completely destroyed by ionic liquids. There is no orderly fibrillar form and compact structure in regenerated WFP. This amorphous structure of regenerated WFP would be beneficial to the

enzymatic hydrolysis.

Enzymatic hydrolysis of IL-regenerated WFP Sugar conversion from WFP during enzymatic hydrolysis

Time dependent sugar conversions during enzymatic hydrolysis of the regenerated WFP are shown in Figure 5. Comparing with native WFP, the sugar conversion of regenerated WFP during enzymatic hydrolysis was significantly increased. The regenerated WFP was almost completely converted to soluble sugars within 7 h (97~99%, Fig. 5), yet the sugar conversion of original WFP was of only ~35%.

The results of enzymatic hydrolysis suggested that regenerated WFP could be digested more efficiently and quickly than the original WFP due to its dominant amorphous regions. It also implied that the higher crystallinities significantly limited the accessibility of cellulases to celluloses and slowed down the reaction rate. Therefore, the high digestibility and hydrolysis rate of regenerated celluloses were attributed to the transformation of the crystalline region to the amorphous region during cellulose dissolution in ILs. Such improvement on cellulose saccharification using an IL-pretreatment step was similar to the results of Dadi.³⁰

In summary, it is possible that the ILs destroy

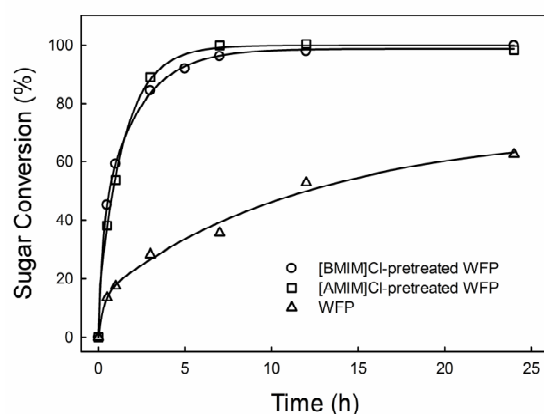


Figure 5: Time-dependent sugar conversion during enzymatic hydrolysis of original and regenerated WFP

the parallel alignment of cellulose molecules derived from hydrogen bonding and the crystalline structure, which exposes much more actively accessible sites to cellulases, resulting in accelerating the reaction rate and an increase of sugar conversion during enzymatic hydrolysis of celluloses.

Time-dependent molecular weight distribution of residues during enzymatic hydrolysis

As shown in Figure 6, the changes in MWD of [BMIM]Cl-pretreated WFP during enzymatic hydrolysis were very fast. For regenerated WFP, there was a broad MWD peak after hydrolysis for 30 s, suggesting a fast decrease of MW (from 4.00×10^5 to 8.00×10^4) and an accumulation of cellulose fractions with various MWs. As the hydrolysis went on (c-g), MWD became narrower and shifted to lower MW (4.00×10^4). It was interesting that after 3 h of hydrolysis (h-i), MWD was always maintained at MW = 4.00×10^4 , only with a decrease in content as the reaction continued.

From the sugar conversion of [BMIM]Cl-pretreated WFP during enzymatic hydrolysis (Fig. 4), it may be noted that even though the hydrolysis was very fast, the conversion could not be completed (to reach 100%). There was still a little cellulose fraction with slightly changed MW hardly digested.

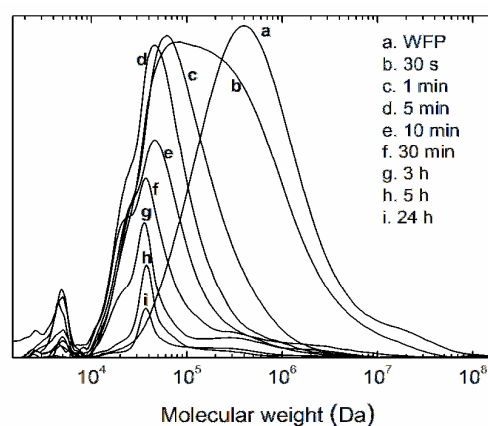


Figure 6: Time-dependent molecular weight distributions of [BMIM]Cl-pretreated WFP during enzymatic hydrolysis

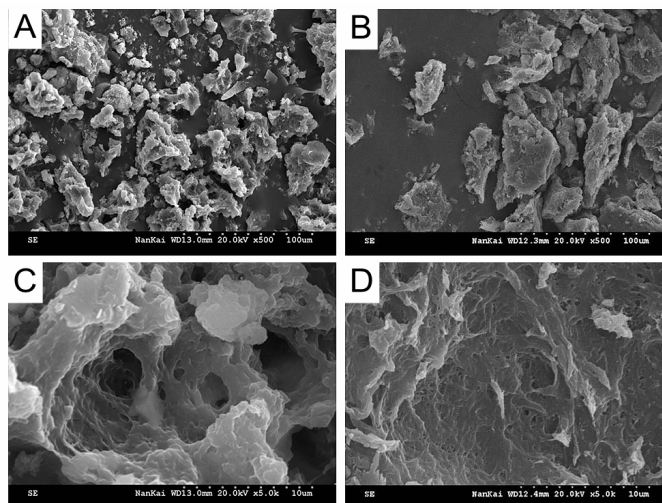


Figure 7: SEM images of regenerated WFP from [AMIM]Cl (A, C) and [BMIM]Cl (B, D) after enzymatic hydrolysis for 24 h (scale bar = 100 μm (A, B) and 10 μm (C, D))

According to the results of some researchers^{39,45} and our former study, it is known that the cleavage on crystalline cellulose by cellobiohydrolases does not result in significant changes in MW. Associated with Figure 6, it could be speculated that the remained fraction with MW of 4.00×10^4 was the crystalline region of the regenerated celluloses. Therefore, this demonstrated that there still was a little amount of crystalline fraction in the regenerated cellulose, which was very difficult to digest

Morphologies of celluloses after enzymatic hydrolysis

After enzymatic hydrolysis for 24 h, a significant fraction of the regenerated cellulose was digested by cellulases, and the filamentous particles were degraded into small pieces (Fig. 7A and 7B) with a shrinking surface (Fig. 7C and 7D). According to the results of Figure 6, the residue of regenerated WFP after 24 h hydrolysis was a crystalline structure. This residue was difficult to degrade, because of its crystalline phase. These SEM results also reflect the difference in the structures of WFP treated with different ILs.²⁸

CONCLUSION

1-Butyl-3-methylimidazolium ([BMIM]Cl) and 1-allyl-3-methylimidazolium chloride

([AMIM]Cl) were synthesized to regenerate Whatman filter paper (WFP) in order to accelerate the enzymatic hydrolysis of cellulose. The reaction rate was significantly improved, with the sugar conversion of nearly 100% after 24 h hydrolysis. For the IL-regenerated WFP, the disappearance of the ordered structure and compact fibrillar morphologies related to the crystalline change (from cellulose I to cellulose II) was noted, which was a major factor enhancing the enzymatic hydrolysis. These results reveal that cellulose biomass can have great potential in biofuel production.

ACKNOWLEDGEMENTS: This work was supported by the Natural Science Foundation of China (NSFC-21006072, 31071509), Natural Science Foundation of Tianjin (No. 15JCYBJC18000), the Beiyang Young Scholar of Tianjin University (2012), and the Program of Introducing Talents of Discipline to Universities of China (No. B06006).

REFERENCES

- ¹ Y. H. P. Zhang and L. R. Lynd, *Biotechnol. Bioeng.*, **88**, 797 (2004).
- ² A. C. O'Sullivan, *Cellulose*, **4**, 173 (1997).
- ³ L. R. Lynd, P. J. Weimer, W. H. van Zyl and I. S. Pretorius, *Microbiol. Mol. Biol. Rev.*, **66**, 506 (2002).
- ⁴ S. M. Notley, B. Pettersson and L. Wagberg, *J.*

- Am. Chem. Soc.*, **126**, 13930 (2004).
- ⁵ Y. Nishiyama, J. Sugiyama, H. Chanzy and P. Langan, *J. Am. Chem. Soc.*, **125**, 14300 (2003).
- ⁶ S. D. Mansfield, C. Mooney and J. N. Saddler, *Biotechnol. Prog.*, **15**, 804 (1999).
- ⁷ A. L. Demain, M. Newcomb and J. H. D. Wu, *Microbiol. Mol. Biol. Rev.*, **69**, 124 (2005).
- ⁸ L. Zhu, J. P. O'Dwyer, V. S. Chang, C. B. Granda and M. T. Holtzaple, *Bioresour. Technol.*, **99**, 3817 (2008).
- ⁹ T. Q. Yuan, W. Wang, L. M. Zhang, F. Xu and R. C. Sun, *Biotechnol. Bioeng.*, **110**, 729 (2013).
- ¹⁰ P. Alvira, E. Tomás-Pejó, M. Ballesteros and M. J. Negro, *Bioresour. Technol.*, **101**, 4851 (2010).
- ¹¹ A. T. W. M. Hendriks and G. Zeeman, *Bioresour. Technol.*, **100**, 10 (2009).
- ¹² M. E. Himmel, S.-Y. Ding, D. K. Johnson, W. S. Adney, M. R. Nimlos *et al.*, *Science*, **315**, 804 (2007).
- ¹³ S. M. Hudson and A. J. Cuculo, *J. Macromol. Sci. Rev. Macromol. Chem. Phys.*, **18**, 1 (1980).
- ¹⁴ C. S. Walseth, *Tappi J.*, **35**, 228 (1952).
- ¹⁵ T. M. Wood and K. M. Bhat, *Methods Enzymol.*, **160**, 87 (1988).
- ¹⁶ K. R. Sharrock, *J. Biochem. Biophys. Methods*, **17**, 81 (1988).
- ¹⁷ R. L. Lamed, R. Kenig, E. Setter and E. A. Bayer, *Enzyme Microb. Technol.*, **7**, 37 (1985).
- ¹⁸ Y. P. Zhang and L. R. Lynd, *Anal. Chem.*, **75**, 219 (2003).
- ¹⁹ Y. P. Zhang, S. Ding, J. R. Mielenz, J. Cui, R. T. Elander *et al.*, *Biotechnol. Bioeng.*, **97**, 214 (2007).
- ²⁰ Y. H. P. Zhang, J. B. Cui, L. R. Lynd and L. R. Kuang, *Biomacromolecules*, **7**, 644 (2006).
- ²¹ C. Kuo and C. Lee, *Bioresour. Technol.*, **100**, 866 (2009).
- ²² D. M. Phillips, L. F. Drummy, D. G. Conrady, D. M. Fox, R. R. Naik *et al.*, *J. Am. Chem. Soc.*, **126**, 14350 (2004).
- ²³ T. Heinze, K. Schwikal and S. Barthel, *Macromol. Biosci.*, **5**, 520 (2005).
- ²⁴ R. P. Swatloski, S. K. Spear, J. D. Holbrey and R. D. Rogers, *J. Am. Chem. Soc.*, **124**, 4974 (2002).
- ²⁵ K. E. Gutowski, G. A. Broker, H. D. Willauer, J. G. Huddleston and R. P. Swatloski *et al.*, *J. Am. Chem. Soc.*, **125**, 6632 (2003).
- ²⁶ J. S. Moulthrop, R. P. Swatloski, G. Moyna and R. D. Rogers, *Chem. Commun.*, **12**, 1557 (2005).
- ²⁷ D. A. Fort, R. C. Remsing, R. P. Swatloski, P. Moyna, G. Moyna *et al.*, *Green Chem.*, **9**, 63 (2007).
- ²⁸ H. Zhang, J. Wu, J. Zhang and J. S. He, *Macromolecules*, **38**, 8272 (2005).
- ²⁹ J. Wu, J. Zhang, J. He, Q. Ren and M. Guo, *Biomacromolecules*, **5**, 266 (2004).
- ³⁰ A. P. Dadi, S. Varanasi and C. A. Schall, *Biotechnol. Bioeng.*, **95**, 904 (2006).
- ³¹ L. Sun, C. L. Li, Z. J. Xue, B. A. Simmons and S. Singh, *RSC Adv.*, **3**, 2017 (2013).
- ³² L. Sun, J. Y. Chen, W. Jiang and V. Lynch, *Carbohydr. Polym.*, **118**, 150 (2015).
- ³³ W. Liu, S. Zhao, L. Li and Z. X. Xin, *Cellulose Chem. Technol.*, **49**, 397 (2015).
- ³⁴ S. Ma, S. J. Yu, Z. H. Wang and X. L. Zheng, *Cellulose Chem. Technol.*, **47**, 527 (2013).
- ³⁵ R. Bodirlau, C. Teaca and I. Spiridon, *Monatsh Chem.*, **141**, 1043 (2010).
- ³⁶ I. Spiridon, C. Teaca and R. Bodirlau, *Bioresources*, **6**, 400 (2010).
- ³⁷ G. Cheng, P. Varanasi, C. Li, H. Liu, Y. B. Melnichenko *et al.*, *Biomacromolecules*, **12**, 933 (2011).
- ³⁸ L. Segal, J. J. Greely, A. E. Martin and C. M. Conrad, *Text. Res. J.*, **8**, 786 (1959).
- ³⁹ H. Pala, M. Mota and F. M. Gama, *Carbohydr. Polym.*, **68**, 101 (2007).
- ⁴⁰ E. Sjöholm, K. Gustafsson, B. Eriksson, W. Brown and A. Colmsjö, *Carbohydr. Polym.*, **41**, 153 (2000).
- ⁴¹ H. G. Higgins, C. M. Stewart and K. J. Harrington, *J. Polym. Sci.*, **51**, 59 (1961).
- ⁴² Y. Takahashi and H. Matsunaga, *Macromolecules*, **24**, 3968 (1991).
- ⁴³ A. Isogai, M. Usuda, T. Kato, T. Uryu and R. H. Atalla, *Macromolecules*, **22**, 3168 (1989).
- ⁴⁴ S. Raymond, A. Kvik and H. Chanzy, *Macromolecules*, **28**, 8422 (1995).
- ⁴⁵ K. M. Kleman-Leyer, M. Siika-Aho, T. T. Teeri and T. K. Kirk, *Appl. Environ. Microbiol.*, **62**, 2883 (1996).